Some comments on shock tube measurements for the initiation and propagation of detonation wave

Rafał Porowski, Andrzej Teodorczyk

Warsaw University of Technology, Institute of Heat Engineering, Nowowiejska 21/25, 00-665 Warsaw, PL

1. Introduction

Shock tube consists of two sections: one called the driver section and the other called the driven or test section [1]. These two sections are filled with gas at different pressures and are initially separated by a thin diaphragm. The pressure in the driver section is greater than in the test section and is slowly increased until the diaphragm ruptures. The rupture of the diaphragm creates a shock wave propagating in the test section and an expansion wave propagating in the driver section, as shown on Fig. 1. The moving boundary between the shock-processed fluid and the expanded fluid is called a contact surface. The conditions across the contact surface are constant pressure and constant velocity. The incident shock wave travels all the way along the test section until it reflects off of the end wall. Similarly, the expansion wave reflects at the end of the driver section. The reflected shock then interacts with either the contact surface or the reflected expansion wave [2].

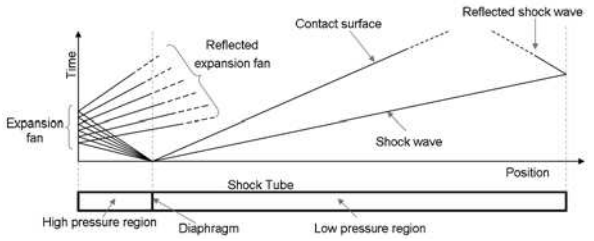

Fig. 1. Shock tube theory and wave propagation diagram. [5]

A very good explanation of the plane shock wave formation was given by Becker [4]. If we imagine a long tube with a piston at the one end (Fig. 2a) and if we let a piston to accelerate with a constant velocity along the tube, which is greater than the sound speed of the gas, the velocity will be reached by the small increments in a short but finite time. The first increment will cause a weak compression wave propagation in the gas at a certain speed (Fig. 2b). The gas between the piston and the wave front will be compressed uniformly and adiabatically. If we let the piston acquire another velocity increment (Fig. 2c) then the second compression wave will be sent out through the moving gas in pursuit of the first if it will travel at a higher velocity relative to the tube. After many such increments the piston will reach its final velocity. At this stage a series of waves of increasing strength will exist between the initial wave and the piston (Fig. 2d). A flow velocity of the gas in the individual waves will increase immediately. Finally, these waves will be able to form a single steep wave front (Fig. 2e), where the large gradients of pressure, density and temperature can be noticed. This is called the shock front moving with high-speed velocity.

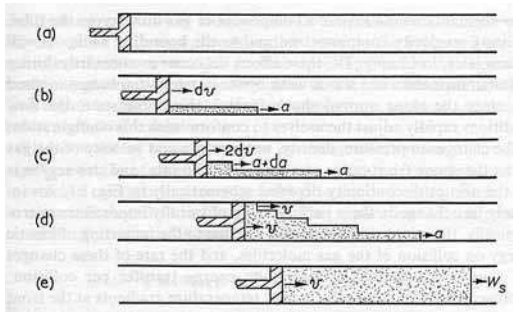

Fig. 2. Schematic model of the shock wave formation. [1]

Any changes in pressure, density, temperature and velocity profiles of the gas across the shock front occur at a fast but finite rate. The fast change in these parameters seems to be physically impossible. From the microscopic perspective, the initial changes in state are due to the imparting of kinetic energy on collision of the gas molecules and the rate of these changes is determined by the finite energy transfer per collision. Considering macroscopic point of view, the infinite velocity and temperature gradients at the front would be counteracted by the large viscous forces and rates of heat conduction [1].

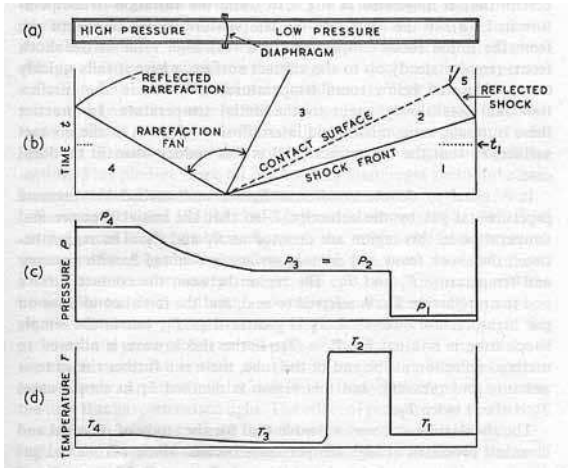

Fig. 3. The X-t diagram of progressing shock wave in the shock tube with the pressure and temperature distributions at time. [1]

A shock wave is a very thin region of the flow across which there is a rapid variation of state. It can almost always be idealized as a surface of discontinuity. This surface propagates into the fluid and all fluid properties: pressure, velocity and density across it are discontinuous. The flow across a shock wave satisfies the conditions of balance for mass, momentum, and energy. Applying these conditions yields the following classical results for a normal shock wave in a perfect gas. The pressure jump, density jump, temperature jump, and velocity jump cross the shock wave are given as well as the Mach number of the flow behind the shock.

Considering above, expansion waves are the continuous changes in the state of a fluid. These waves propagate relative to the fluid at the speed of sound. They tend to spread and the change in properties across them is smooth. The fluid is expanded and accelerated in the direction opposite to the direction of propagation of the wave. Most importantly, expansion waves are isentropic, which is not the case for a shock. In the shock tube problem, we will have to deal only with expansion fans, which are series of waves starting from a common space-time location. The flow across an expansion fan can be solved using the method of characteristics. It uses invariants along characteristics going across the expansion fan. A Prandtl-Meyer expansion fan is a centered

expansion process, which turns a supersonic flow around a convex corner. The fan consists of an infinite number of Mach waves, diverging from a sharp corner. In case of a smooth corner, these waves can be extended backwards to meet at a point. Each wave in the expansion fan turns the flow gradually (in small steps). Across the expansion fan, the flow accelerates (velocity increases) and the Mach number increases, while the static pressure, temperature and density decrease. Since the process is isentropic, the stagnation properties remain constant across the fan [2,6].

In the shock tube technology, diaphragms are in common use to separate a driver section from driven one. Diaphragms are usually chosen according to the strength of the shock front and should be designed for the so-called "bursting pressure" which is depended on the mechanical properties of diaphragm material (e.g. aluminum, steel copper, nickel, etc.). The bursting processes can be perform either naturally under an increasing pressure [1,8] or hydraulically by operating plunger as was described by Gould [9].

When a diaphragm is allowed to burst naturally a fundamental question is: what is a variation of the bursting pressure with the diaphragm thickness and diameter? Natural bursting pressure for a diaphragm made from a particular material is proportional to its thickness and inversely proportional to its exposed diameter [1, 8]. Table 1 shows some diaphragm materials and their bursting characteristics. If the values of bursting pressures are known then the linear relation will allow extrapolation over the rest of the pressure range in the shock tube.

The shock wave formation combining with a supersonic chemically reacting flow can be easily found in the detonation phenomenon for combustible gaseous mixtures. According to characteristic features of the detonation process given by Lee and Moen [13], the phenomenon of detonation propagation can be generally divided in two phases, in particular:

- creation of conditions for the onset of detonation by processes of flame acceleration, vorticity production, formation of jets and mixing of products and reactants,
- formation of the detonation wave itself or the onset of detonation.

Tab. 1. Selected diaphragm materials and their bursting characteristics. [1,8]

Diaphragm material	Thickness [mm]	Tube diameter [mm]	Bursting pressure [bar]	References
Cellophane	0.02	25.4	1.52	Henshall (1957)
Polyethylene	0.05	76.2	3.24	Henshall (1957)
Copper	0.19	31.75	34.47	East (1960)
Copper	0.25	31.75	55.16	East (1960)
Copper	0.41	31.75	89.63	East (1960)
Copper	0.56	31.75	131.00	East (1960)
Copper	0.68	31.75	165.47	East (1960)
Aluminum	0.04	63.5	1.59	Gaydon (1963)
Aluminum	0.1	63.5	4.48	Gaydon (1963)
Aluminum	0.15	63.5	7.03	Gaydon (1963)
Aluminum	0.25	63.5	10.34	Gaydon (1963)
Aluminum	0.3	63.5	13.44	Gaydon (1963)
Aluminum	0.81	81.28	27.58	East (1960)
Aluminum	1.62	81.28	55.16	East (1960)
Aluminum	1.27	31.75	110.32	East (1960)
Aluminum	1.57	31.75	137.89	East (1960)
Nickel	0.09	76.2	43.92	Schultz and Henshall (1957)
Nickel	0.38	76.2	64.19	Schultz and Henshall (1957)
Steel S.3	1.78	444.5	206.84	Hufton (1957)

Numerous experimental studies and accidents in the industry have shown that if a combustible gaseous mixture is not too close to the flammability limits then a flame propagation in an obstacle area can accelerate very rapidly to high supersonic velocities. Such high-speed flame can drive shock waves with substantial overpressures.

If the mixture is sufficiently sensitive, the highly accelerated flame my undergo transition to detonation. It was shown by Lee [14] that the smaller a cell size the more detonation sensitive is the mixture. Depending on the fuel concentration and initial and geometrical conditions, steady flame propagation in obstructed tube progresses in the one of following regimes [10,15]:

- flame quenching – flame fails to propagate,
- subsonic low-velocity flame – flame propagates at a speed much lower than the speed of sound in the combustion products,
- CJ deflagration – high-speed flame propagating with the velocity close to the speed of sound in the combustion products (600 – 1200 m s^{-1}),
- quasi-detonation – flame propagates with the velocity between the speed of sound in the combustion products and the CJ value,
- DDT and detonation – flame velocity is close to CJ value.

Our goal was to observe the propagation of the shock-induced detonation wave using different gaseous mixtures in the driver section and the influence on the pressure and velocity of the propagating and reflecting detonation in the driven section of the shock tube.

2. Experimental set-up

Our shock tube has a total length of 6.8 m. The driven section is consisted of four sub-sections (2 x 2 m and 2 x 1 m) jointed together with inner diameter of 140 mm and 6 m long. The driver section is 0.8 m long with inner diameter equal to 90 mm. We performed our experiments using stoichiometric hydrogen-air mixtures in the driven section at initial pressure of 1 atm and temperature of 293 K and both stoichiometric acetylene-oxygen and stoichiometric hydrogen-oxygen mixtures filled in the driver section at 0.5 atm and also temperature of 293 K. Fig. 4 shows schematically our experimental set-up and Fig. 5 presents some pictures of our shock tube.

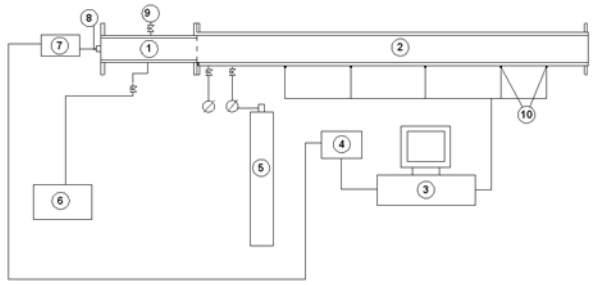

Fig. 4. Experimental set-up, where: 1 – driver-section tube; 2 – driven-section channel; 3 – PC and data acquisition system; 4 – time sequencer; 5 – hydrogen-methane-air cylinder; 6 – pomp; 7 – ignition device; 8 – ignitron plug; 9 – dillution valve; 10 – pressure transducers and ion probes.

The driver and driven sections were separated by a thin aluminum diaphragm A1-Z4 and 0.75 mm thick. The flame propagation and pressure wave were monitored along the driven section by pressure transducers and ion probes.

Fig. 5. Some pictures of our shock tube.

Pressure transducers were located at different positions along the channel to collect data concerning the detonation development. To validate our experimental results from the shock tube we did some calculations of CJ and ZND parameters using CANTERA open-source and Matlab and we found both results in a good agreement.

3. Results and discussion

Using the standard PCB gauges located along the driven section of our shock tube we collected data about the propagation velocities of the detonation wave. To initiate a combustion process in driver section we used a weak ignition source – an electrical plug. After ignition both acetylene-oxygen and hydrogen-oxygen mixtures broke a diaphragm and a shock induced a tested mixture let the combustion process accelerate and form a detonation wave in the driven section. Both acetylene-oxygen mixture and hydrogen-oxygen mixture detonate in the driver section before the diaphragm bursting. A rapid pressure increase at the shock front for both mixture broke the diaphragm and let the hydrogen-air mixture detonate also. Before our experiments we did some thermodynamic calculations of our tested mixture.

Computations were done with CANTERA open-source and MATLAB software for the CJ and ZND parameters of the stoichiometric hydrogen-air mixture. For example, the CJ velocity for our experimental set-up (P_0 = 1 atm, T_0 = 293 K) is equal to 1974 m s^{-1} (Fig. 6).

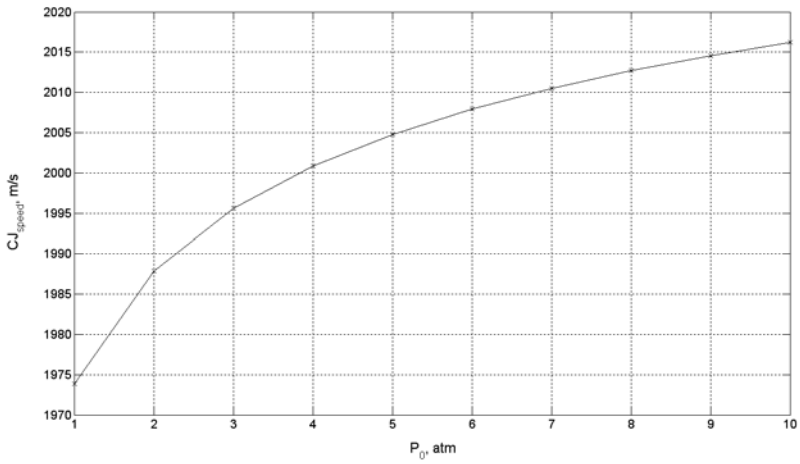

Fig. 6. Detonation CJ velocities for stoichiometric hydrogen-air mixture vs. initial pressures of the mixture, calculated by CANTERA open-source and MATLAB software.

Comparing this CJ value to the calculated CJ velocity in the driver section, for stoichiometric acetylene-oxygen mixture (2420 m s^{-1}) or hydrogen-oxygen mixture (2020 m s^{-1}), we should expect the similar velocities taken from experiments. As we noticed, our experimental data are quite different than computational results.

Tab. 2. Experimental data concerning velocities in the driven section from the shock tube.

Tested mixture: stoichiometric hydrogen-air mixture, P_1 = 1 bar **Driver mixture:** stoichiometric hydrogen-oxygen, P_1 = 0.5 bar						
Test no.	Δt_1 [μs]	Δt_2 [μs]	Δt_3 [μs]	V_1 [m s^{-1}]	V_2 [m s^{-1}]	V_3 [m s^{-1}]
01	254.2	127.1	124.0	1968.5	1968.5	2016.1
02	251.1	127.1	127.1	1992.0	1968.5	1968.5
03	254.2	124.0	127.1	1968.5	2016.1	1968.5

Tab. 3. Experimental data concerning velocities in the driven section from the shock tube.

Tested mixture: stoichiometric hydrogen-air mixture, P_1 = 1 bar **Driver mixture:** stoichiometric acetylene-oxygen, P_1 = 0.5 bar						
Test no.	Δt_1 [μs]	Δt_2 [μs]	Δt_3 [μs]	V_1 [m s^{-1}]	V_2 [m s^{-1}]	V_3 [m s^{-1})]
01	235.6	124.0	124.0	2122.2	2016.1	2016.1
02	257.3	127.1	130.2	1943.2	1966.9	1920.1
03	232.5	117.8	120.9	2122.2	2122.2	2067.8

Tables 2 and 3 give us some details regarding detonation velocities of the stoichiometric hydrogen-air mixture in the driven section induced by both hydrogen-oxygen and acetylene-oxygen mixtures in the driver section. Data are chosen from three repeatable tests in both cases. We can observe that detonation velocities in the driven section initiated by the acetylene-oxygen mixture are slightly higher than in other case. A reasonable explanation of this fact can be either the higher CJ velocity and pressure of acetylene-oxygen mixture or the higher detonation sensitivity [14] of this mixture itself rather than hydrogen-oxygen mixture. If we look at Fig. 7, we can easily find that there are some "common" point at the velocities profiles in the driven section. This point was noticed at a distance of 5250 mm from the ignition point. At this point the propagating detonation wave was stable and the velocity was comparable to the calculated CJ value.

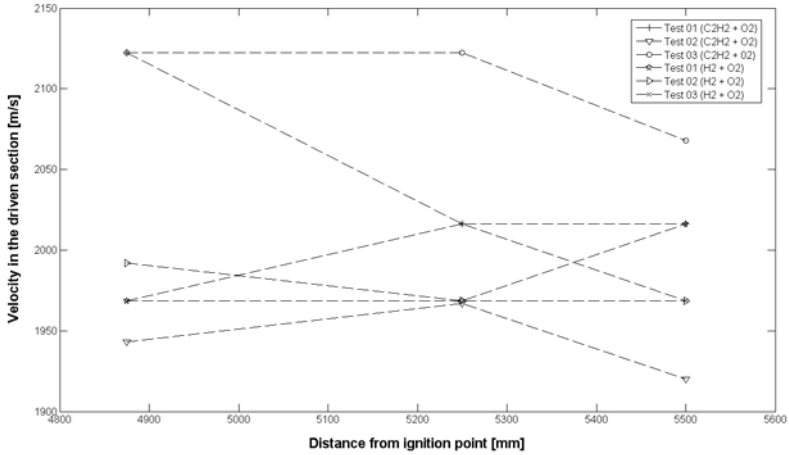

Fig. 7. Velocity profiles at the driven section in the shock tube. Red lines: driver section with stoichiometric acetylene-oxygen mixture, driven section with stoichiometric hydrogen-air mixture. Blue lines: driver section with stoichiometric hydrogen-oxygen mixture, driven section with stoichiometric hydrogen-air mixture.

We also did some computations using CANTERA and MATLAB on ZND parameters for detonating stoichiometric hydrogen-air mixture with the shock front propagating with CJ speed. Fig. 8 shows some data obtained from our calculations. For our tested mixture the maximum pressure at the travelling shock front reached a value of 27.1 atm and then decreased to 14.8 atm. For the temperature profile we observe a rapid growth up to max. 2952.8 K.

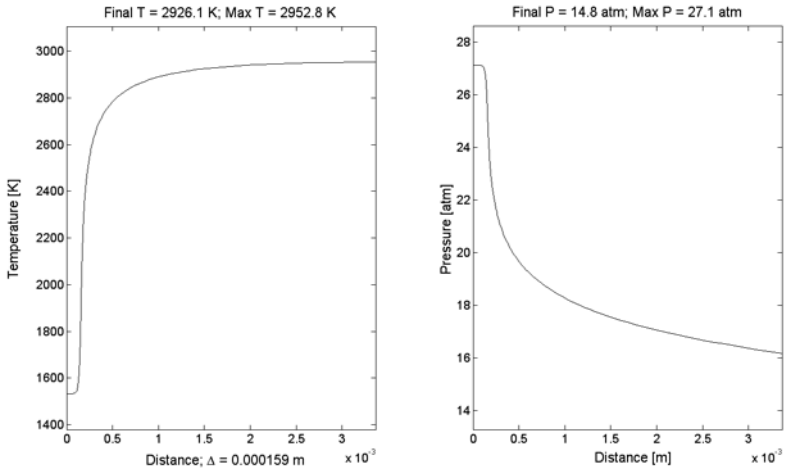

Fig. 8. Pressure and temperature profiles for detonating stoichiometric hydrogen-air mixture with the shock front propagating with CJ speed.

According to our results shown at Fig. 9 the maximum experimental pressure at the propagating shock front in the driven section was slightly higher than calculated value, reaching about 31.5 atm. This pressure value was observed at the same distance where the detonation wave reached a stable propagating regime. The same distance (5125 mm) from the ignition point, as in the velocity measurements, was a so-called run-up distance for the onset of detonation in our experiments. The propagating detonation wave became a stable at the time close to 1.25 ms traveling more than 5 m from the initiation moment. The last pressure gauge located at the distance about 5.6 m recorded the arrived shock front at the time close to 1.5 ms leaving a distance about 0.4 m from the end of our shock tube.

Due to a shock front reflection from the closed end of the tube we noticed a classical Taylor expansion wave [15]. Taylor expansion wave in the detonation phenomenon can be explained as following [16]. Product gases behind the onset of detonation expand isentropically and then accelerate. This makes a high distribution of particle velocities. This distribution was investigated in details by G.I. Taylor. This theory provides a possibility to predict the velocity decay behind the CJ detonation wave. If look at Fig. 9 we can see the Taylor expansion waves for a single pressure records obtained in the driven section. For the last pressure gauge record at the distance about 5.6 m from ignition point we can observe the expansion wave lasting about 0.5 ms and then pressure at the shock front immediately rises up to the value slightly below the state just before the wave reflected from the tube wall. This is the case where the reflected shock wave is the strongest. Analyzing other pressure records (coming back from the last one) we notice that the Taylor waves are longer and consequently reflected shock wave propagating backward is slower with the pressure reaching below 19 atm at distance about 4.6 m from ignition point.

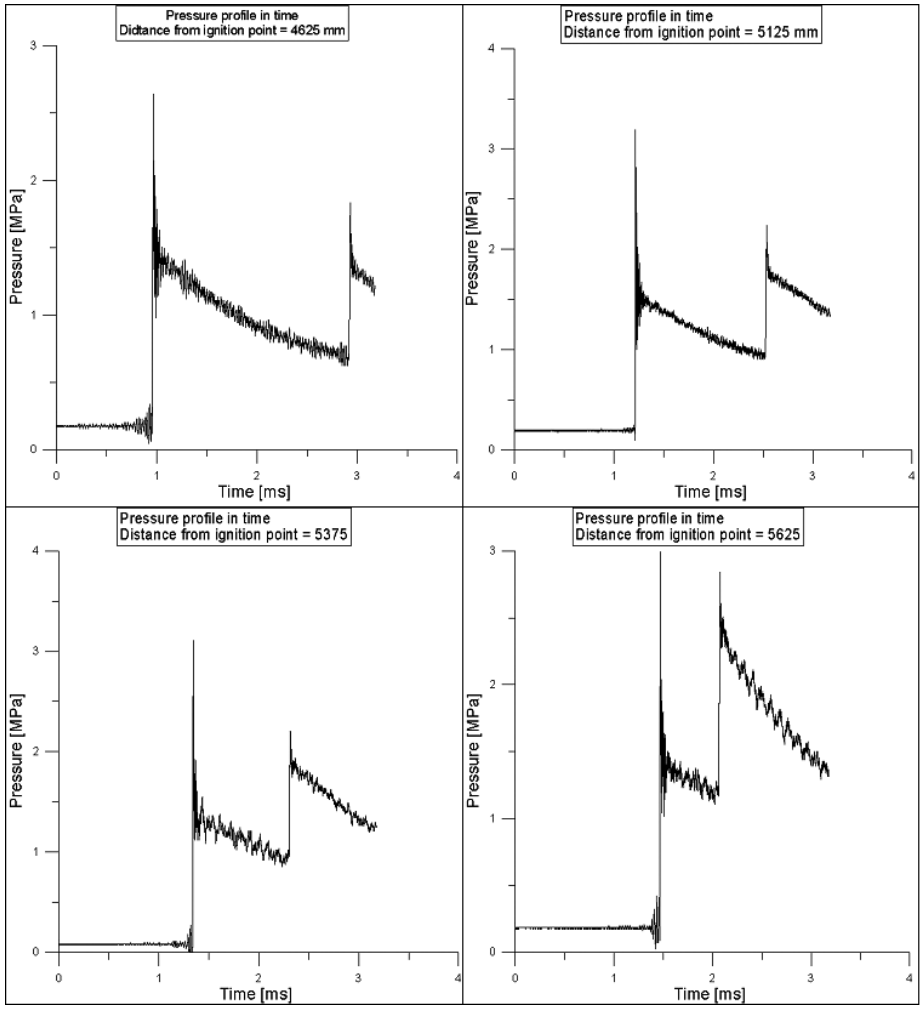

Fig. 9. Single pressure profiles for stoichiometric hydrogen-air mixture at the driven section in the shock tube. Driver section was filled with stoichiometric acetylene-oxygen mixture.

The shock-induced initiation process that can place in the classical shock tube in the detonation theory can be determined as the ignition via turbulent mixing. In that case it is extremely difficult to model theoretically since it involves many processes including turbulent mixing, shock waves and chemical reactions simultaneously. Experimentally, it is also difficult to obtain a detailed, quantitative observation of the gas dynamics and chemical processes in the mixing zone at the head of the jet. Thus, it is of value to analyze some simple theoretical limiting cases to deduce some qualitative information on the jet initiation phenomenon. We shall assume the hot inert gas (initially at the constant volume state) to first expand isentropically to M = 1. Then we shall investigate the non-equilibrium chemical reactions when different amounts of unburned mixtures are mixed with the expanded hot inert gas. By computing the temperature after mixing, T_m the induction time, τ, and the adiabatic temperature, T_a after mixing of hot inert gas and unburned mixtures for different mixing volume ratio, $R = \upsilon_{jet} / \upsilon_u$, we can gain some insight into most favorable conditions for ignition process of combustible mixtures.

The jet parameters of hot inert gas can be estimated with the assumption of sonic (M = 1) and isentropic flow. The temperature and pressure at the jet exit cross section are equal to, respectively:

$$\frac{T_{jet}}{T_r} = \frac{2}{\gamma + 1}$$

$$\frac{P_{jet}}{P_r} = \left(\frac{2}{\gamma + 1} \right)^{\frac{\gamma}{\gamma - 1}}$$

Where P_r and T_r are the pressure and temperature of gas in driven section of the experimental setup behind reflected shock wave, T_{jet} and P_{jet} are temperature and pressure of gas at the exit from orifice. Next, we shall assume that the given volume of expanded hot inert gas υ_{jet} to be mixed simultaneously with a certain volume of cold unburned combustible mixture υ_u (at room temperature). The temperature after constant pressure adiabatic mixing T_m can readily be determined from energy conservation, i.e.

$$\rho_{jet}\, \upsilon_{jet}\, C_{p_{jet}} T_{jet} + \rho_u\, \upsilon_u\, C_{p_u} T_u = \left(\rho_{jet} \upsilon_{jet} C_{p_{jet}} + \rho_u\, \upsilon_u\, C_{p_u} \right) T_m$$

And solving for T_m gives:

$$T_m = T_{jet} \left(\frac{1}{1 + \left(\frac{\rho_u C_{p_u}}{\rho_{jet} C_{p_{jet}}} \right) \frac{1}{R}} \right) + T_u \left(\frac{1}{1 + \left(\frac{\rho_{jet} C_{p_{jet}}}{\rho_u C_{p_u}} \right) R} \right)$$

Where $R = \upsilon_{jet} / \upsilon_u$ is the volume ratio of the given volume of hot inert gas to unburned cold combustible mixtures in the mixing zone. Knowing T_m the ignition induction time τ and adiabatic temperature T_a after reaction of mixed inert gas and combustible mixture can be determined using of CANTERA and MATLAB software.

4. Conclusions

Our goal was to adopt the classical shock tube technique for the experimental investigation of the propagating shock-induced detonation wave. We used different gaseous mixtures in the driver section, namely both stoichiometric hydrogen-oxygen and acetylene-oxygen mixtures. The driven section was filled only with stoichiometric hydrogen-air mixture. An influence of the driver section mixture on the pressure and velocity of the propagating and reflected detonation wave in the driven section of the shock tube was investigated experimentally and computationally. We found some interesting observations and correlations between calculated results and experimental data. Calculated pressure and velocity values for tested mixture are in a quite good agreement with our shock tube results for the propagating detonation wave. We also tried to give some theoretical introduction on modeling the shock-induced initiation process that can place in the classical shock tube.

Literature

[1] Gaydon A.G., Hurle I.R., *The shock tube in high-temperature chemical physics*, Chapman and Hall LTD, 1963.

[2] Liepmann H., Roshko A., *Elements of Gas Dynamics*. GALCIT Aeronautical Series. Wiley and Sons, 1957.

[3] Petersen E., Hanson R., *Nonideal effects behind reected shock waves in a high-pressure shock tube*, Shock Waves, 10/2001.

[4] Becker R., 1922, Z. Phys., 8, 321.

[5] http://en.wikipedia.org/wiki/Shock_tube
[6] Shapiro, Ascher H., *The Dynamics and Thermodynamics of Compressible Fluid Flow*, Vol. 1, Ronald Press.
[7] Liepmann H., Bowman R., *Shape of shock fronts in shock tubes.* Physics of Fluids, 7(12):2013{2015, 1964.
[8] Ferri A., *Fundamental data obtained from shock-tube experiments,* Pergamon Press, 1961.
[9] Gould D.G., UTIA Report, Inst. Of Aerophysics, University of Toronto, 1952.
[10] Teodorczyk A., Chapter 8.4 in Jarosiński J., Veyssiere B., *Combustion phenomena. Selected mechanisms of flame formation, propagation and extinction*, CRC Press, 2009.
[11] Zel'dovich Ya. B., Raizer Yu. P., *Physics of shock waves and high-temperature hydrodynamic phenomena,* Dover Publications Inc., 2002.
[12] Piskorek A., *Podstawy matematyczne propagacji fal uderzeniowych,* 2003.
[13] Lee J.H.S., Moen I.O., *The mechanism of transition from deflagration to detonation in vapour cloud explosion*, Progress in Energy and Combustion Science, 6, 1980.
[14] Lee J.H.S., Ng H.D., Comments on explosion problems for hydrogen safety, Journal of Loss Prevention in the Process Industries, 21, 2008.
[15] Lee J.H.S., *The detonation phenomenon,* Cambridge, 2008.
[16] Mannan S., *Lee's Loss Prevention in the Process Industries*, Vol. 2, 3rd Edition, Elsevier, 2005.